

# Isothermal crystallization kinetics, morphology, and thermal conductivity of graphene nanoplatelets/polyphenylene sulfide composites

Shuling Deng · Zhidan Lin · Baofeng Xu ·  
Weiping Qiu · Kunyu Liang · Wei Li

Received: 28 February 2014 / Accepted: 13 June 2014 / Published online: 24 July 2014  
© Akadémiai Kiadó, Budapest, Hungary 2014

**Abstract** Graphene nanoplatelets (GNP) and polyphenylene sulfide (PPS) were used as filler and matrix, respectively, to produce composites. The PPS/GNP thermal composites were prepared via a melt blending method. The effects of GNP on crystallization behavior and kinetics, morphology, and thermal properties of PPS/GNP composites were investigated. To determine the isothermal crystallization kinetics parameters and isothermal crystallization activation energy, the Avrami model was used to comparatively analyze the relevant DSC experimental data. The results show that GNP provides an obvious heterogeneous nucleation effect on PPS to accelerate the crystallization and decrease isothermal crystallization activation energy. Thermal conductivity values of PPS/GNP composites with various GNP contents revealed that GNP remarkably increases thermal conductivity of composites mainly via a layered dispersion in PPS matrix. Thermal conductivity also increased with increasing GNP content, which was further improved at elevated temperatures. The thermal conductivities of PPS composite containing 30 mass% of GNP were 1.156 and 1.350 W m<sup>-1</sup> K<sup>-1</sup> at 30 and 110 °C, respectively, indicating an increase of more than 3 times compared with the neat PPS.

**Keywords** Polyphenylene sulfide (PPS) · Graphene nanoplatelets (GNP) · Crystallization · Nucleation · Thermal conductivity · Composites

## Introduction

Polyphenylene sulfide (PPS), with a rigid chemical structure, is composed of phenyl groups linked by sulfur atoms. It is a semicrystalline thermoplastic engineering polymer. Because of stiff structure, it offers good thermal stability, chemical resistance, flame resistance, precision moldability, and excellent frictional properties. The outstanding characteristics of PPS make it widely popular in various applications, including electronics and electrical appliances, automobile, precision instruments, chemical sector, and aerospace [1, 2]. However, the application of neat PPS has been limited due to its relatively low glass transition temperature (~90 °C), compared with its high melting temperature (~275 °C) and narrow processing temperature range, brittleness, and low strength. Therefore, PPS is mostly compounded with other polymers [3–5] or rigid particles [6–14] to overcome these disadvantages.

Graphene is an atomically thick two-dimensional (2D) sheet composed of *sp*<sup>2</sup> carbon atoms arranged in a honeycomb structure. It has attracted great research interest due to its double traits [15–20] of graphite and carbon nanotube, such as large specific surface area (2,630 m<sup>2</sup> g<sup>-1</sup>) [15], low price and remarkable mechanical properties (with Young's modulus of 1 TPa and ultimate strength of 130 GPa) [16], thermal conductivity (5,000 W m<sup>-1</sup> K<sup>-1</sup>) [17], and electrical properties (electron mobility up to 200,000 cm<sup>2</sup> V<sup>-1</sup> s<sup>-1</sup> at room temperature) [18]. Thus, GNP, viewed as a new high-performance reinforcing nanomaterial, can bring a wide range of improvements to the polymer composites. In this work, PPS composites with improved mechanical and thermal properties were prepared via compounding GNP and PPS. At present, the related researches mainly focus on improving the mechanical performance, thermal, and electrical conductivity of PPS composites via mixing graphene

S. Deng · Z. Lin (✉) · B. Xu · W. Qiu · K. Liang · W. Li  
College of Science and Engineering, Jinan University,  
Guangzhou 510632, People's Republic of China  
e-mail: linzd@jnu.edu.cn

**Table 1** Composition of the PPS/GNP composites in mass%

Sample	PPS	GNP
PPS	100	–
PPS/GNP1	99	1
PPS/GNP5	95	5
PPS/GNP10	90	10
PPS/GNP20	80	20
PPS/GNP30	70	30

nanoplatelets (GNP) and PPS. Whereas, studies indicated that GNP also exhibits nucleation effect on the crystallization of semicrystalline polymers [21, 22]. For crystalline polymers, the strength, dimensional stability, wear resistance, and some other characters of material depend on its crystallization behavior, crystalline morphology, and degree of crystallinity [23]. Therefore, the study of isothermal crystallization kinetics of PPS matrix is helpful to understand the relationship between crystallization rate and temperature. According to crystallization parameters, such as Avrami exponent, half-time of crystallization, and crystallization rate, we can better understand mechanism of formation of nuclei and crystalline growth of polymers. The study on this subject is very important from both theoretical and practical views. In this paper, we examined the influence of GNP on the isothermal melt crystallization behavior and thermal conductivity of PPS, and analyzed its variation, using a differential scanning calorimetry (DSC) technique.

## Experimental

### Materials

PPS-HB, with degree of crystallinity of 5 %, relative density of  $1.3 \text{ g cm}^{-3}$ , was obtained from Deyang Science and Technology Company, PR China. GNP sample (KNG-180, with diameter of  $40 \mu\text{m}$ , thickness less  $100 \text{ nm}$ ) was supplied by Xiamen Knano Graphene Technology, People's Republic of China.

### Preparation of PPS/GNP composites

After adequately drying in a vacuum oven at  $80 \text{ }^\circ\text{C}$  for 24 h, PPS and GNP were homogenized and compounded in a twin-screw extruder according to the compositions presented in Table 1 to obtain PPS/GNP composite with various GNP contents. The extrusion temperatures for compounding were set between  $220$  and  $290 \text{ }^\circ\text{C}$  and the screw speed at  $120 \text{ rpm}$ . In this article, PPS/GNP composites are denoted as PPS/GNP; for example, PPS with 1 mass% GNP is denoted as PPS/GNP1.

### DSC characterization

A Q200 DSC (TA Instruments Ltd, Crawley, West Sussex, UK) was used to study the thermal behavior of PPS/GNP composites. Samples of 8–9 mg were accurately weighed for DSC examinations. All measurements were performed in a nitrogen atmosphere.

For isothermal crystallization behavior characterization, a composite sample was heated to  $320 \text{ }^\circ\text{C}$  for 5 min to eliminate the previous thermal history. Then, it was cooled to the desired crystallization temperature ( $T_c$ ) of 248, 250, 252, 254, or  $256 \text{ }^\circ\text{C}$  at a rate of  $100 \text{ }^\circ\text{C min}^{-1}$  and held for a certain period of time until the crystallization was completed. It is important to mention that each sample was used only once in DSC examinations.

### Morphology examination

The specimens, which were broken in the impact property examinations, were used for morphology studies. The fracture surfaces of the specimens were sputter coated with gold before conducting microscopic examinations with a Philips XL-30 environmental scanning electron microscope (ESEM) at an acceleration voltage of  $20 \text{ kV}$ .

### The thermal conductivity

Thermal conductivity of composite materials was examined in temperature range of  $30$ – $110 \text{ }^\circ\text{C}$  using Netzsch LFA 427 instrument according to laser flash method [24, 25].

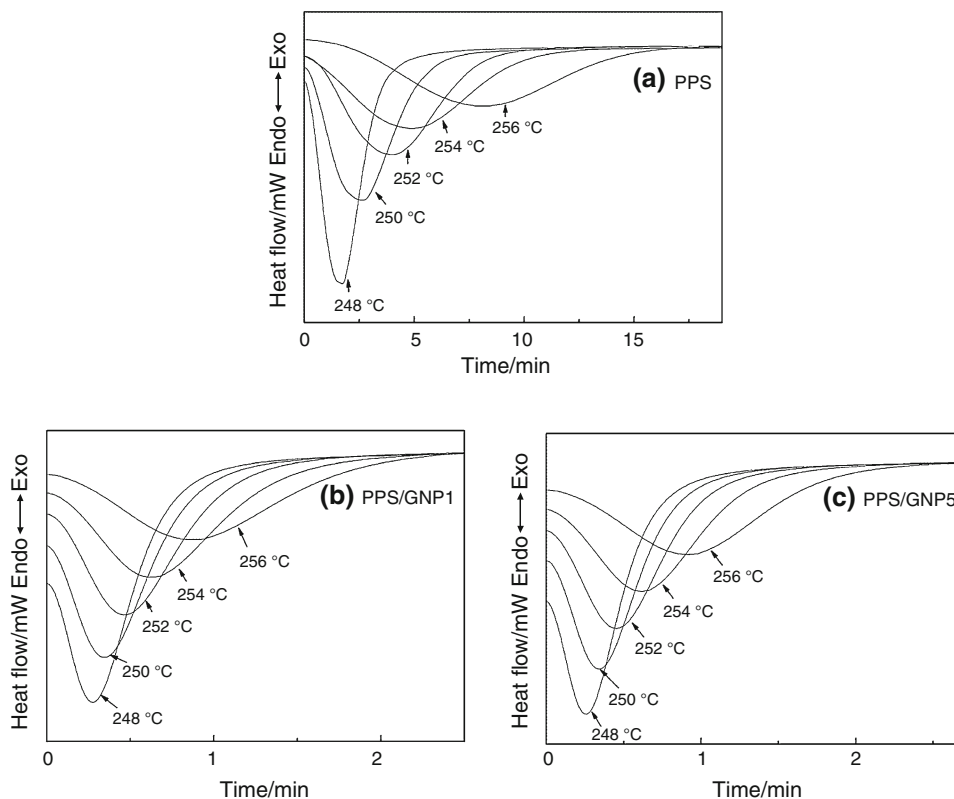
## Results and discussion

### Isothermal crystallization kinetics

Figure 1 shows the isothermal crystallization curves of PPS and PPS composites containing 1 and 5 mass% of GNP crystallizing at various temperatures. As Fig. 1 reveals, the broader crystallization peaks appeared at higher crystallization temperature ( $T_c$ ) and longer time required to complete crystallization.

At the same crystallization temperature, the addition of GNP obviously reduced the total time of crystallization. It has great influence on the crystallization behavior of composite with only introducing 1 mass% GNP. It is assumed that the variation in crystallization can be attributed to the special structures of GNP. The larger specific surface area of GNP produces a large interaction interface with the polymeric matrix, so that GNP particles provide strong adsorptive effects to PPS chains and a nucleation effect on PPS, acting as a nucleating agent. This effect shortens the crystallization

**Fig. 1** Isothermal crystallization curves of PPS and PPS/GNP composites at different temperature



induction period, improves crystallization rate, and reduces time to complete crystallization.

The overall isothermal melt crystallization kinetics of neat PPS and its composites with various GNP loadings were further analyzed using the well-known Avrami equation [26–28]

$$X_t = 1 - \exp(-kt^n), \tag{1}$$

where  $X_t$  is the relative crystallinity at crystallization time  $t$ ,  $k$  is crystallization rate constant involving both nucleation and growth rate parameters, and  $n$  is the Avrami exponent depending on the nature of nucleation and growth geometry of the crystals. The double-logarithmic form of the Avrami equation is as follows:

$$\ln[-\ln(1-X_t)] = \ln k + n \ln t, \tag{2}$$

$X_t$  is the relative crystallinity at crystallization time  $t$ , which can be calculated according to Eq. (3)

$$X_t = \int_{t_0}^t (dH_c/dt) \int_{t_0}^{t_\infty} (dH_c/dt) dt, \tag{3}$$

where  $t_0$  is the initial crystallization time,  $t_\infty$  is infinite time, and  $dH_c/dt$  is the heat evolution rate. From a plot of  $\ln[-\ln(1 - X_t)]$  versus  $\ln t$ , a straight line is obtained. The Avrami exponent  $n$  and crystallization kinetic constant  $k$  are determined from the slope and intersection of the

straight line, respectively. The half-time of PPS crystallization ( $t_{1/2} = (\ln 2/k)^{1/n}$ ) is defined as the time at which  $X(t)$  is 50%. The reciprocal of  $t_{1/2}$  can be used to characterize the crystallization rate

$$G_{1/2} = 1/t_{1/2}. \tag{4}$$

According to Eq. (3), the development of the relative crystallinity with time for isothermal crystallization of PPS and its composites is shown in Fig. 2. The half-time of PPS crystallization ( $t_{1/2}$ ) can be determined conveniently from plots in Fig. 2. These diagrams show that the crystallization time is prolonged with increasing  $T_c$  in both samples. In addition, the crystallization time becomes shorter in the composites than in neat PPS. These results indicate that the presence of GNP accelerated the isothermal melt crystallization of PPS in the PPS/GNP composites.

Using diagrams of Fig. 2, plots of  $\ln[-\ln(1 - X_t)]$  versus  $\ln t$  at the same cooling rates for the neat PPS and its composites were drawn (Fig. 3). The obtained values of kinetic parameters of  $t_{1/2}$ ,  $G_{1/2}$ ,  $k$ , and  $n$  are listed in Table 2. The plots show linear relationship throughout the crystallization process, indicating that the Avrami equation is suitable for describing the isothermal crystallization behavior of these nanocomposites. However, they later deviate from the linear relationship, which suggests that the actual crystallization process of PPS nanocomposites is more complicated than the model presented by Avrami

**Fig. 2** Plots of relative crystallinity versus crystallization time for **a** neat PPS, **b** PPS/GNP1, and **c** PPS/GNP5 during isothermal melt crystallization

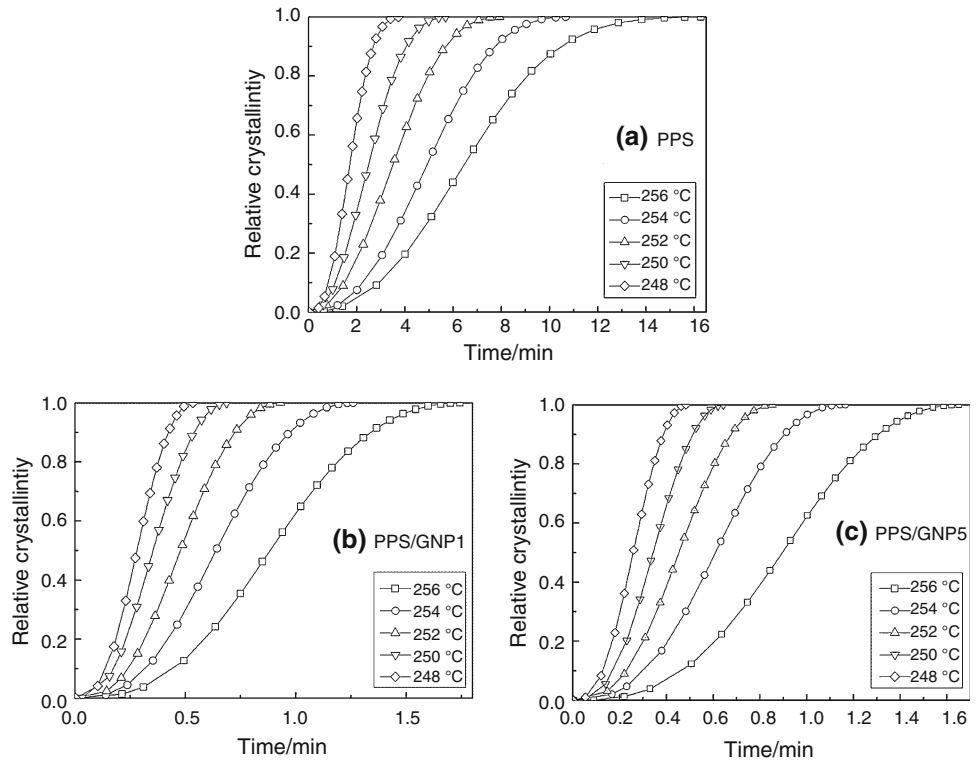
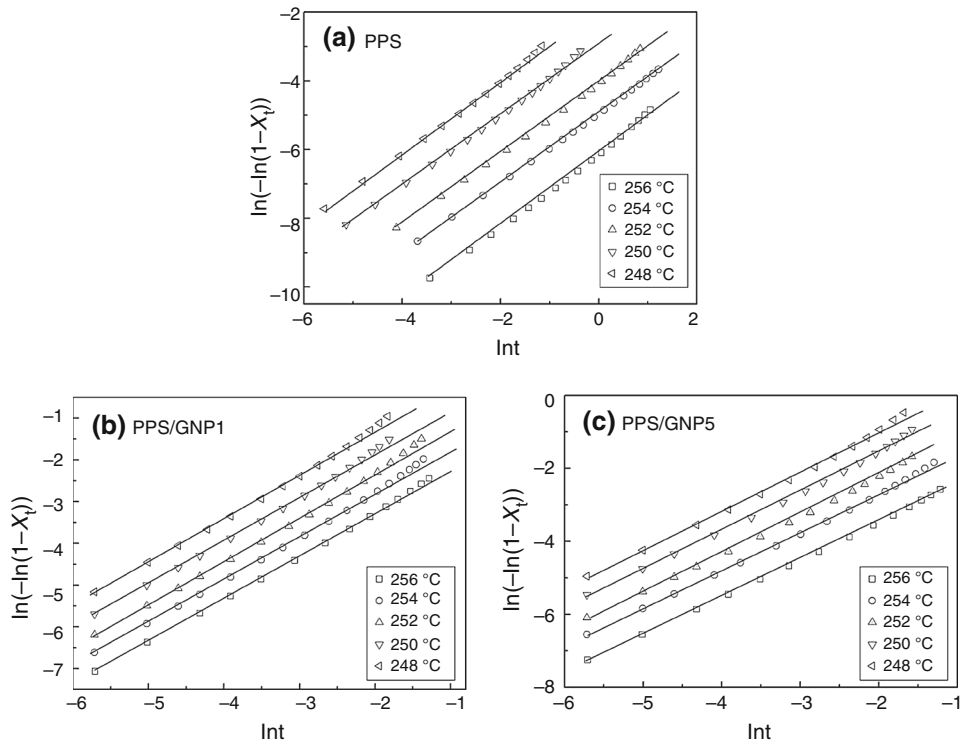


**Fig. 3** Avrami curves of PPS and PPS/GNP composites isothermally crystallized at different temperatures



equation. This behavior can be attributed to the fact that GNP as a nanomaterial with large specific surface area, high surface energy, and easy reunion characters affects the crystallization rate of PPS in the composites.

The kinetic parameters of  $n$  and  $k$  for neat PPS and composites are presented in Table 2. The Avrami exponent  $n$  is related to the type of nucleation and growth geometry of the crystals. As shown in Table 2, the  $n$  values of neat

**Table 2** Kinetic parameters of PPS and PPS/GNP composites

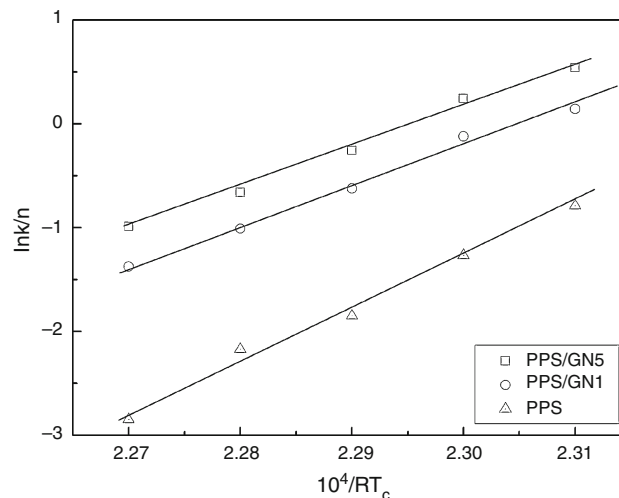
Samples	$T_c/^\circ\text{C}$	$n$	$k/\text{min}^{-n}$	$t_{1/2}/\text{min}$	$G_{1/2}/\text{min}^{-1}$	$\Delta E/\text{kJ mol}^{-1}$
PPS	248	1.10	0.9950	1.69	0.592	478.12
	250	1.07	0.0631	2.48	0.403	
	252	1.00	0.0427	4.03	0.248	
	254	1.02	0.0282	4.92	0.203	
	256	1.04	0.0132	6.46	0.155	
PPS/GNP1	248	1.01	1.5574	0.28	3.571	373.95
	250	0.84	1.1584	0.35	2.857	
	252	1.02	0.7153	0.48	2.083	
	254	1.04	0.4757	0.64	1.563	
	256	1.07	0.3166	0.88	1.136	
PPS/GNP5	248	1.00	1.7177	0.26	3.846	377.91
	250	1.04	1.2892	0.34	2.941	
	252	1.11	0.7520	0.46	2.174	
	254	1.01	0.5107	0.61	1.639	
	256	1.04	0.3584	0.86	1.163	

PPS and PPS/GNP composites ranged from 1.00–1.10 to 0.84–1.11, respectively, which means that the nucleation mechanism was not modified significantly in the PPS/GNP composites at the examined  $T_c$  range. It can be observed from the data that the crystallization rate constant  $k$  of PPS decreased with increasing crystallization temperature, an indication of a strong dependence of  $k$  on the crystallization temperature. The crystallization rate constant  $k$  of PPS/GNP composites also decreased with increasing crystallization temperature, but at smaller degree than that of neat PPS. This observation suggests that PPS/GNP composites are less sensitive to temperature than PPS due to presence of GNP particles in the polymer. It is clear from the data presented in Table 2 that  $G_{1/2}$  decreases, whereas  $t_{1/2}$  increases with increasing  $T_c$  for all the three samples, indicating a slow-down of the isothermal crystallization rate at higher  $T_c$ . It is because the macromolecular chains with great exercise capacity become more difficult to be fixed with increasing  $T_c$ , resulting in prolonging crystallization time. Table 2 obviously shows that, at a given  $T_c$ ,  $G_{1/2}$  is greater in composites than in neat PPS, whereas  $G_{1/2}$  is greater in PPS/GNP5 than in PPS/GNP1 composite. Therefore, it can be concluded that the isothermal melt crystallization process of PPS is gradually accelerated in composites with increasing the GNP content owing to the heterogeneous nucleation effect.

#### Isothermal crystallization activation energy

According to the Arrhenius model, crystallization activation energy can be expressed as Eq. (5)

$$k^{1/n} = k_0 \exp[-(E_2 - E_1)/RT_c], \quad (5)$$

**Fig. 4** Relationships between  $\ln k/n$  and  $1/RT_c$  of PPS and composite materials

where  $E_2$  is crystalline state energy,  $E_1$  is melt state energy,  $k_0$  is pre-exponential factor,  $R$  is the gas constant, and  $T_c$  is crystallization temperature. Substituting crystallization activation energy  $\Delta E$  for  $E_1 - E_2$  and taking logarithms on both sides of Eq. (5), one obtains

$$\ln k/n = \ln k_0 + \Delta E/RT_c. \quad (6)$$

Plotting  $\ln k/n$  against  $1/RT_c$  gives straight lines (Fig. 4). The values of  $\Delta E$  were calculated from the slopes of the straight lines (Table 2). The obtained values of  $\Delta E$  for neat PPS, PPS/GNP1, and PPS/GNP5 samples were 478.12, 373.95, and 377.91  $\text{kJ mol}^{-1}$ , respectively. As these values indicate,  $\Delta E$  of neat PPS is much greater than those of composite samples. Moreover, the  $\Delta E$  of PPS/GNP5 was found greater than that of PPS/GNP1. This observation reveals that the existence of large amounts of GNP in the PPS matrix may reduce the mobility of PPS segments due to the large surface area and special nanostructures of GNP. Generally, the  $\Delta E$  of PPS composites exhibited a decreasing trend with introducing GNP particles. This suggests that, as the crystallization progressed, it is easier for polymer to crystallize, which once again proved that GNP acts as an effective nucleating agent for PPS.

#### Thermal properties of PPS/GNP composites

The SEM micrographs in Fig. 5 illustrate the morphologies of PPS and PPS/GNP composites containing 5, 10, and 30 mass% GNP. Figure 5a, b reveals that GNP particles were uniformly dispersed in the PPS matrix and wrapped by PPS matrix resin. The two phases were integrated tightly, but they did not have a high degree of interconnection, resulting in less thermal path. Figure 5c, d

**Fig. 5** SEM images of **a** PPS, **b** PPS/GNP5, **c** PPS/GNP10, and **d** PPS/GNP30 composites

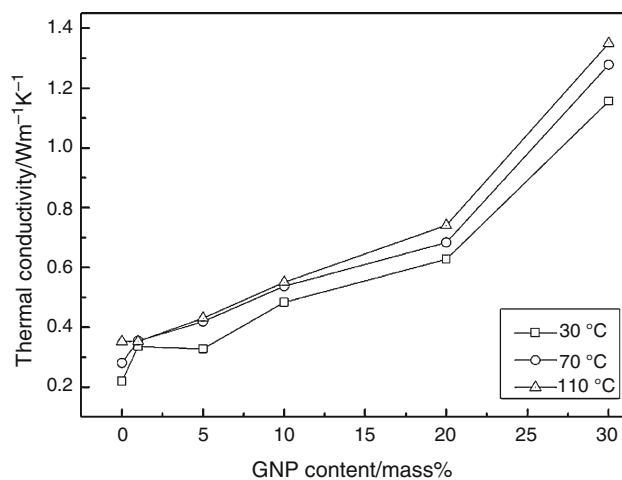
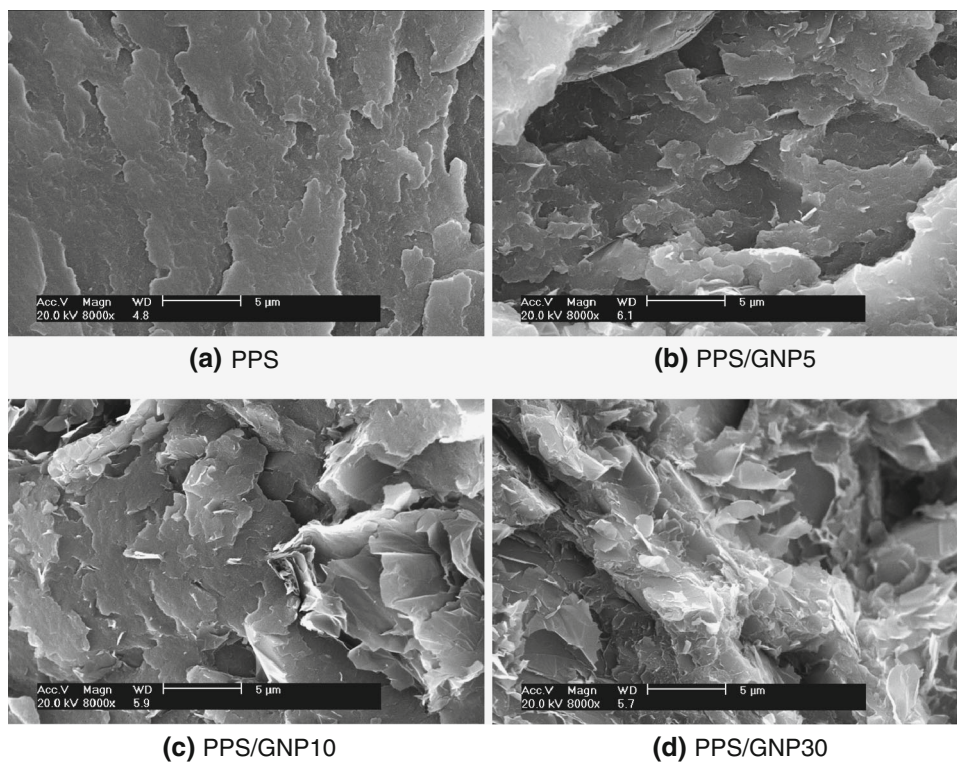


**Fig. 6** Values of  $k_{\text{eff}}$  for PPS/GNP composites

evidences that the impact fracture surface became rough with increasing the GNP content through a layered dispersion in PPS matrix. In addition, GNP particles aggregate on the surface of matrix when the filler content in the composite reach 30 mass%. As shown in Fig. 6, thermal conductivities of PPS/GNP30 composite at different temperatures rise more rapidly, showing formation of a relatively complete thermal network at this point.

Figure 6 plots the effective thermal conductivities ( $k_{\text{eff}}$ ) of GNP reinforced PPS composites at various temperatures. In

the diagrams, at the same filler content,  $k_{\text{eff}}$  increased when temperature increased. Moreover, at the same temperature,  $k_{\text{eff}}$  of composites basically exhibited an increasing trend. When the GNP particle content in the composite reached 5 mass%, the  $k_{\text{eff}}$  can be improved stably. Especially, when the particle content increased to more than 20 mass%, the  $k_{\text{eff}}$  greatly improved. Results revealed that the largest  $k_{\text{eff}}$  was achieved when PPS was loaded with 30 mass% of GNP. The GNP promoted the thermal conductivity of the neat PPS ( $0.219 \text{ W m}^{-1} \text{ K}^{-1}$ ) by about fivefold ( $1.156 \text{ W m}^{-1} \text{ K}^{-1}$ ) at 30 °C, whereas promoted the thermal conductivity of the neat PPS ( $0.352 \text{ W m}^{-1} \text{ K}^{-1}$ ) by about threefold ( $1.350 \text{ W m}^{-1} \text{ K}^{-1}$ ) at 110 °C. These phenomena may be described based on large surface area and higher aspect ratio of GNP particles [29]. The large surface area was beneficial to promote more polymer-filler interaction that facilitates heat conduction. Moreover, the high aspect ratio was beneficial to promote the interconnectivity among filler particulates.

## Conclusions

The crystallization, morphology, and thermal properties of PPS in PPS/GNP composites prepared via a melt blending process were strongly influenced by GNP. DSC analysis suggested that GNP accelerates the crystallization and decreases isothermal crystallization activation energy of PPS in the composites due to the strong heterogeneous

nucleation effect of GNP particles. The results were interpreted using Avrami model that successfully describes the isothermal crystallization kinetics. The presence of a high GNP content in PPS matrix remarkably increased thermal conductivity of composites mainly via a layered dispersion. Moreover, thermal conductivity of composites can be further improved with the increase in examination temperature. The largest  $k_{\text{eff}}$  at different temperatures was attained through adding 30 mass% of GNP to PPS, which all promoted the thermal conductivity of the neat PPS by above threefold. Therefore, good performance PPS/GNP thermal composites were successfully prepared through using industrialized GNP as thermal filler at a reasonable cost.

**Acknowledgements** This project was supported by Major Science and Technology Projects of Guangdong Province, China (Grant No. 2012A080106009).

## References

- Schuster M, De Araujo CC, Atanasov V, Andersen HT, Kreuer KD, Maier J. Highly sulfonated poly (phenylene sulfone): preparation and stability issues. *Macromolecules*. 2009;42:3129–37.
- Yang J, Xu T, Lu A, Zhang Q, Tan H, Fu Q. Preparation and properties of poly(phenylene sulfide)/multiwall carbon nanotube composites obtained by melt compounding. *Compos Sci Technol*. 2009;69:147–53.
- Kalkar A, Deshpande V, Kulkarni M. Isothermal crystallization kinetics of poly (phenylene sulfide)/TLCP composites. *Polym Eng Sci*. 2009;49:397–417.
- Zou H, Ning N, Su R, Zhang Q, Fu Q. Manipulating the phase morphology in PPS/PA66 blends using clay. *J Appl Polym Sci*. 2007;106:2238–50.
- Guo Y, Bradshaw RD. Isothermal physical aging characterization of polyether-ether-ketone (PEEK) and polyphenylene sulfide (PPS) films by creep and stress relaxation. *Mech Time-Depend Mater*. 2007;11:61–89.
- Wu D, Wu L, Zhou W, Yang T, Zhang M. Study on physical properties of multiwalled carbon nanotube/poly(phenylene sulfide) composites. *Polym Eng Sci*. 2009;49:1727–35.
- Noll A, Burkhart T. Morphological characterization and modeling of electrical conductivity of multi-walled carbon nanotube/poly(*p*-phenylene sulfide) nanocomposites obtained by twin screw extrusion. *Compos Sci Technol*. 2011;71:499–505.
- Cho MH, Bahadur S. A study of the thermal, dynamic mechanical, and tribological properties of polyphenylene sulfide composites reinforced with carbon nanofibers. *Tribol Lett*. 2007;25:237–45.
- Zou H, Xu W, Zhang Q, Fu Q. Effect of alkylammonium salt on the dispersion and properties of Poly (*p*-phenylene sulfide)/clay nanocomposites via melt intercalation. *J Appl Polym Sci*. 2006;99:1724–31.
- Saito T, Okamoto M, Hiroi R, Yamamoto M, Shiroi T. Intercalation of diphenyl sulfide into nanogalleries and preparation of poly(*p*-phenylenesulfide)-based nanocomposites. *Macromol Mater Eng*. 2006;291:1367–74.
- Liang J, Liu G. Effects of nano-CaCO<sub>3</sub> content and surface treatment on tensile properties of PPS/GF ternary composites. *Polym-Plast Technol*. 2006;26:60–3.
- Yang Y, Duan H, Zhang S, Niu P, Zhang G, Long S, Wang X, Yang J. Morphology control of nanofillers in poly (phenylene sulfide): a novel method to realize the exfoliation of nanoclay by SiO<sub>2</sub> via melt shear flow. *Compos Sci Technol*. 2013;75:28–34.
- Naffakh M, Marco C, Gómez MA, Gómez-Herrero J, Jiménez I. Use of inorganic fullerene-like WS<sub>2</sub> to produce new high-performance polyphenylene sulfide nanocomposites: role of the nanoparticle concentration. *J Phys Chem B*. 2009;113:10104–11.
- Flores A, Naffakh M, Díez-Pascual AM, Ania F, Gómez-Fatou MA. Evaluating the reinforcement of inorganic fullerene-like nanoparticles in thermoplastic matrices by depth-sensing indentation. *J Phys Chem C*. 2013;117:20936–43.
- Stoller MD, Park S, Zhu Y, An J, Ruoff RS. Graphene-based ultracapacitors. *Nano Lett*. 2008;8:3498–502.
- Lee C, Wei X, Kysar J, Hone J. Measurement of the elastic properties and intrinsic strength of monolayer graphene. *Science*. 2008;321:385–8.
- Bolotin KI, Sikes KJ, Jiang Z, Klima M, Fudenberg G, Hone J, Stormer HL. Ultrahigh electron mobility in suspended graphene. *Solidstate Commun*. 2008;14:351–5.
- Balandin AA, Ghosh S, Bao W, Calizo I, Teweldebrhan D, Miao F, Lau CN. Superior thermal conductivity of single-layer graphene. *Nano Lett*. 2008;8:902–7.
- Patsidis AC, Kalaitzidou K, Psarras GC. Graphite nanoplatelets/polymer nanocomposites: thermomechanical, dielectric, and functional behavior. *J Therm Anal Calorim*. 2014;116:41–9.
- Jeong SG, Jeon J, Chung O, Kim S, Kim S. Evaluation of PCM/diatomite composites using exfoliated graphite nanoplatelets (xGNP) to improve thermal properties. *J Therm Anal Calorim*. 2013;114:689–98.
- Zhang F, Peng XC, Yan WB, Peng ZY, Shen YQ. Nonisothermal crystallization kinetics of in situ nylon 6/graphene composites by differential scanning calorimetry. *J Polym Sci Part B*. 2011;49:1381–8.
- Xu JZ, Chen C, Wang Y, Tang H, Li ZM, Hsiao BS. Graphene nanoplatelets and shear flowation crystallization in isotactic polypropylene nanocomposites. *Macromolecules*. 2011;44:2808–18.
- Auer C, Kalinka G, Krause T, Hinrichsen G. Crystallization kinetics of pure and fiber-reinforced poly(phenylene sulfide). *J Appl Polym Sci*. 1994;51:407–13.
- Cha J, Seo J, Kim S. Building materials thermal conductivity measurement and correlation with heat flow meter laser flash analysis and TCI. *J Therm Anal Calorim*. 2012;109:295–300.
- Hay B, Filtz JR, Hameury J, Rongione L. Uncertainty of thermal diffusivity measurements by laser flash method. *Int J Thermophys*. 2005;26:1883–98.
- Avrami M. Kinetics of phase transition 2. Transformation time relations. *J Chem Phys*. 1940;8:212–24.
- Avrami M. Granulation, phase change, and microstructure kinetics of phase change 3. *J Chem Phys*. 1941;9:177–84.
- Sidel SM, Santos FA, Gordo VO, Idalgo E, Monteiro AA, Moraes JC, Yukimitu K. Avrami exponent of crystallization in tellurite glasses. *J Therm Anal Calorim*. 2011;106:613–8.
- Khan MO, Leung SN, Chan E, Naguib HE, Dawson F, Adinkrah V. Effects of microsized and nanosized carbon fillers on the thermal and electrical properties of polyphenylene sulfide based composites. *Polym Eng Sci*. 2013;53:2398–406.